Lariat capping as a tool to manipulate the 5′ end of individual yeast mRNA species in vivo

NICOLAI KROGH,[1] MAX PIETSCHMANN,[1] MANFRED SCHMID,[2] TORBEN HEICK JENSEN,[2] and HENRIK NIELSEN[1]

[1]Department of Cellular and Molecular Medicine, University of Copenhagen, DK-2200 Copenhagen N, Denmark
[2]Department of Molecular Biology and Genetics, Aarhus University, 8000 Aarhus C, Denmark

ABSTRACT

The 5′ cap structure of eukaryotic mRNA is critical for its processing, transport, translation, and stability. The many functions of the cap and the fact that most, if not all, mRNA carries the same type of cap makes it difficult to analyze cap function in vivo at individual steps of gene expression. We have used the lariat capping ribozyme (LCrz) from the myxomycete *Didymium* to replace the mRNA m^7G cap of a single reporter mRNA species with a tiny lariat in which the first and the third nucleotide are joined by a 2′, 5′ phosphodiester bond. We show that the ribozyme functions in vivo in the budding yeast *Saccharomyces cerevisiae* presumably without cofactors and that lariat capping occurs cotranscriptionally. The lariat-capped reporter mRNA is efficiently exported to the cytoplasm where it is found to be oligoadenylated and evenly distributed. Both the oligoadenylated form and a lariat-capped mRNA with a templated poly(A) tail translates poorly, underlining the critical importance of the m^7G cap in translation. Finally, the lariat-capped RNA exhibits a threefold longer half-life compared to its m^7G-capped counterpart, consistent with a key role for the m^7G cap in mRNA turnover. Our study emphasizes important activities of the m^7G cap and suggests new utilities of lariat capping as a molecular tool in vivo.

Keywords: lariat capping ribozyme; mRNA processing; m^7G; polyadenylation; mRNA turnover

INTRODUCTION

The m^7GpppN cap structure of eukaryotic mRNA 5′ ends plays a critical role in many aspects of gene expression, including mRNA splicing, polyadenylation, export, translation initiation, and overall stability (Topisirovic et al. 2011; Gonatopoulos-Pournatzis and Cowling 2014; Ramanathan et al. 2016). Given this plethora of functions, it is experimentally attractive to dissect the role of the cap in distinct cellular processes by manipulating its structure, preferably on individual mRNA. However, present strategies to this end have shortcomings. Genetic interference with cap synthesis affects all mRNA and inhibits cell growth, making it difficult to distinguish direct from indirect effects caused by the mutation. As an alternative, switching the promoter to redirect mRNA transcription from RNA polymerase (RNAP) II to RNAPIII is a possibility, but along with changed cap status, RNAPIII transcription also affects pre-mRNA splicing and 3′ end formation restricting its applicability. Finally, insertion of a *cis*-cleaving ribozyme (Dower et al. 2004; Meaux and Van Hoof 2006), or the recognition sites for the endonucleases RNase III (Meaux et al. 2011) or RNase P, leaves the post-

cleaved 3′ fragment with either a 5′ OH (small ribozymes) or 5′ monophosphate (RNase III or RNase P). Transcription using bacteriophage RNA polymerases creating RNA triphosphate 5′ ends is also possible (Dower and Rosbash 2002). These RNA 5′ends are all substrates for cellular enzymes that will result in 5′–3′ degradation hampering any functional studies.

We have previously described the naturally occurring lariat capping ribozyme (LCrz; formerly GIR1), that caps a homing endonuclease mRNA in several eukaryotic microorganisms, including myxomycetes and amoeboflagellates (Nielsen et al. 2008; Tang et al. 2011, 2014). LCrz cleaves in *cis* at an internal processing site (IPS) by branching, leaving the downstream fragment with a 5′ lariat in which the first and the third nucleotide are linked by a 2′, 5′ phosphodiester bond (Nielsen et al. 2005; Meyer et al. 2014). This structure is referred to as a lariat cap and appears to substitute for all functions of a conventional mRNA cap in the native system (Vader et al. 1999). The ribozyme and the homing endonuclease gene are located together in a group I intron in the

SSU rRNA gene and the lariat capping mechanism is viewed as an adaptation to expression of a mRNA from within a RNAPI gene (Johansen et al. 2007).

Ribozymes can be transferred to non-native organisms and have been used as experimental tools to study RNA processing and gene expression in bacterial, fungal, and mammalian systems (Sullenger and Gilboa 2002; Long et al. 2003). LCrz is active in vitro in the absence of protein cofactors and hence likely to be transferable. LCrz has the additional advantage that the lariat cap is resistant to cellular 5′–3′ degradation activities when expressed ectopically. Specifically, the lariat cap is not a substrate for cellular debranching enzymes (Nielsen et al. 2005) and the particular structure of the lariat cap (Meyer et al. 2014), including the absence of an exposed 5′ end, makes it unlikely to be a substrate for decapping enzymes and 5′–3′ exonucleases. Thus, transplantation of LCrz may be used to create stable transcripts in which the m^7G cap is missing, exposing its roles in mRNA metabolic processes.

Here, we transfer LCrz to *S. cerevisiae* and explore its impact on the processing, localization, expression, and stability of a GFP reporter mRNA. We find that the ribozyme efficiently cleaves the precursor transcript during transcription and that the lariat-capped mRNA (LC-GFP mRNA) is efficiently exported to the cytoplasm. The LC-GFP mRNA is threefold more stable compared to a conventionally capped GFP mRNA (m^7G-GFP mRNA), accumulates to high levels in an oligoadenylated form, and is translated, albeit with very low efficiency. Thus, we confirm that stabilization against degradation and stimulation of translation are the major roles of the native cap. Understanding of lariat cap behavior in cells may reveal new aspects of gene expression and have potential for biotechnological application.

RESULTS

Production of LC-GFP mRNA in *S. cerevisiae*

To study the biological activity of the lariat cap in *S. cerevisiae*, we fused the LCrz upstream of cDNA encoding GFP and inserted the construct into the expression plasmid pG-1 (Fig. 1A). The specific version of LCrz used was "Di-166.22," meaning the ribozyme from *Didymium iridis*, comprising 166-nt upstream and 22-nt downstream, respectively, of the internal processing site (IPS). In pG-1, transcription is driven by the constitutive glyceraldehyde-3-phosphor dehydrogenase (GPD) promoter and 3′ end formation by the phosphoglycerate kinase (PGK) terminator. Three variants of the construct were made: (i) the experimental construct containing the wt LCrz (LC-GFP) and expected to produce the lariat-capped GFP mRNA; (ii) a positive control (m^7G-GFP), that incorporates only the 22 nt of the ribozyme that are found downstream from the IPS and an additional 21-nt upstream of this sequence that were included for technical reasons; and (iii) a negative expression control (LCmut-GFP), containing LCrz carrying a single point mutation (G174C) that is known from in vitro studies to completely inactivate the ribozyme (Decatur et al. 1995). The mRNA produced from the positive control construct (m^7G-GFP
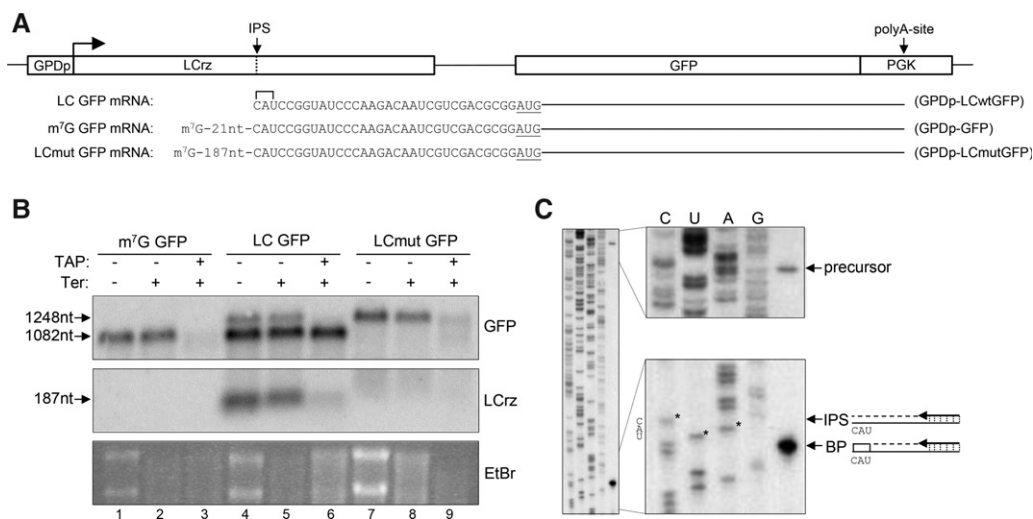

FIGURE 1. Expression of a lariat-capped mRNA. (*A*) Schematic illustration of the basic experimental construct and the three variant mRNAs with mRNA denominations to the *left* and construct names to the *right*. For technical reasons, the m^7G GFP control mRNA incorporates an additional 21 nt of transcribed vector sequence (5′-AGAACUUAGUUCGACGGAUCC; the full sequences are found in Supplemental Material). (*B*) Northern blotting analysis of experimental and control reporters from whole cell RNA treated with (+) or without (−) Tobacco Acid Pyrophosphatase (TAP) and Terminator exonuclease (Ter). The Northern membrane was hybridized with a probe against GFP (*top* panel) or a probe against LCrz (*middle* panel). Only relevant parts of the membrane are shown. EtBr staining of LSU and SSU rRNA was included as loading control and to show Ter degradation of RNA with a 5′-phosphate (*bottom* panel). The expected size of RNAs detected is indicated. (*C*) Primer extension analysis of experimental and control reporters from whole cell RNA run next to a sequencing ladder. Primer extension stop signals corresponding to the 5′ end of the precursor transcript and the branch point (BP), respectively, can be observed. No signal is observed at the position corresponding to hydrolytic cleavage at the internal processing site (IPS).

mRNA) carries a conventional m^7G cap and an initiation codon in a similar sequence context as the experimental LC-GFP constructs mRNA. The mRNA produced by the LCmut-GFP negative control is similar to LC-GFP except that it harbors a 200-nt long 5′ UTR consisting of the mutated ribozyme sequence with multiple start codons in two reading frames and stop codons present in all three reading frames (Supplemental Fig. S1).

Expression of the three constructs was first studied by Northern blotting analysis of whole cell RNA. Using a probe targeting the GFP part of the mRNA, we observed single bands of the expected sizes derived from both of the m^7G-GFP and LCmut-GFP controls (Fig. 1B, lanes 1,7). For the experimental LC-GFP construct (lane 4), two bands were observed. The upper band corresponds to the precursor transcript as deduced by its co-migration with the LCmut-GFP control, while the lower band corresponds to the presumed 3′ cleavage product as deduced by its migration close to the size of the m^7G-GFP control. Hybridization with a probe targeting the ribozyme part of the mRNA revealed the expected 5′ cleavage product in the experimental lanes only (Fig. 1B, lanes 4–6). Thus, we conclude that LCrz cleaves the transcript in vivo and the ~1:4 ratio of precursor to 3′ cleavage product indicates that cleavage is relatively efficient. LC-GFP mRNA levels were four- to fivefold and eight- to 10-fold higher than those of the m^7G-GFP and LCmut-GFP samples, respectively, as evidenced by phosphoimager analysis of the Northern blot (data not shown). Since transcription was driven from the same promoter and RNA was isolated from parallel cultures, this indicates that the LC-GFP mRNA is more stable than its conventionally capped m^7G-GFP mRNA counterpart.

LCrz is known from in vitro experiments to catalyze not only the lariat capping branching reaction as described above but also hydrolytic cleavage yielding a 5′-monophosphate on the downstream fragment (Nielsen et al. 2005). Cleavage in the native system of *Didymium* cells occurs exclusively by branching (Vader et al. 1999). We carried out two different types of analysis to distinguish between these possibilities in the present experiment. First, we probed the nature of the 5′ ends of the assayed mRNAs by enzymatic treatment, using tobacco acid pyrophosphatase (TAP) to convert 5′ tri-phosphates and m^7G-caps to 5′ monophosphates in combination with Terminator exonuclease (Ter) digesting only RNA with 5′ monophosphates. RNA resulting from such treatments was analyzed by Northern blotting hybridization. A 3′ fragment derived from hydrolytic cleavage should be removed by Ter alone whereas a lariat-capped 3′ fragment should be resistant. Similarly, the conventional m^7G cap should only be removed by the combined TAP/Ter treatment, whereas the lariat cap again should be resistant. As shown in Figure 1B (lanes 2,5,8), all mRNAs resisted Ter treatment. Moreover, the m^7G-GFP mRNA, the LCmut-GFP mRNA, the 5′ end fragment derived from LCrz cleavage and the uncleaved LC-GFP precursor transcript were all

sensitive to TAP + Ter treatment (Fig. 1B, lanes 3,6,9), as expected for m^7G-capped RNAs. In contrast, the LC-GFP mRNA (Fig. 1B, lane 6, GFP Northern) survived TAP+Ter treatment, strongly indicating that its cleavage had occurred by the branching reaction. A similar conclusion was reached when we mapped the cleavage site by primer extension analysis. RNA that is cleaved by branching will result in premature primer extension stop signals because the branch acts as an efficient block to the reverse transcriptase (Nielsen et al. 2005). Consistent with the Northern result, only the stop signals corresponding to the precursor 5′ end and the branch nucleotide were observed (Fig. 1C). Thus, LC-GFP mRNA is efficiently produced from our experimental construct and LCrz cleavage occurs exclusively by branching. This implies that LCrz is transferable from *Didymium* to yeast.

LC-GFP mRNAs are oligoadenylated at steady state

Having established that the experimental LC-GFP mRNA is lariat capped, we next analyzed its polyadenylation status by an RNase H/oligo(dT) assay (Fig. 2A). RNase H cleaves the RNA in RNA:DNA hybrids and removes the poly(A) tail in an oligo(dT)-dependent fashion, resulting in a mobility shift on Northern gels. We also used an upstream DNA oligo to shorten the interrogated RNAs and thereby increase the resolution of the assay. Figure 2B shows the Northern blotting analysis of our three transcripts with parallel samples with (+) or without (−) oligo(dT) in the RNase H reactions. For both of the control transcripts, a clear shift from diffuse signals (lanes 1,5) to distinct and faster migrating species (lanes 2,6) was observed. This demonstrates the expected polyadenylation of these m^7G-capped transcripts. The LC-GFP mRNA displayed both a diffuse signal and a distinct band in RNase H assays excluding oligo(dT) (lane 3), which collapsed into a single, faster migrating distinct band upon oligo(dT) addition (lane 4). We interpret the diffuse signal to derive from the uncleaved precursor transcript observed previously (Fig. 1B, lane 4) based on its co-migration with the signal in lane 5. The distinct band, on the other hand, constitutes the bulk of the signal and most likely reflects the lariat-capped mRNAs, which consequently harbor only short poly(A) tails (Fig. 2B, note the slight change in migration between lanes 3 and 4).

The absence of a long poly(A) tail on the LC-GFP mRNA could be due to deficient polyadenylation, increased deadenylation, or an unusual stability of deadenylated RNA. To gain more information on these possibilities, we expressed the m^7G- and LC-GFP constructs in a strain deleted for the major cytoplasmic deadenylase Ccr4p (Tucker et al. 2001) and in a strain with an additional deletion of the Pan2p poly(A) nuclease (Brown and Sachs 1998). Using the RNase H/oligo(dT) assay, poly(A) tails of m^7G-GFP mRNAs appeared considerably longer in the double *ccr4Δpan2Δ* mutant compared to its corresponding wt strain (compare mobility differences in lanes 1 and 2 in Fig. 2B and Fig. 2C, respectively).
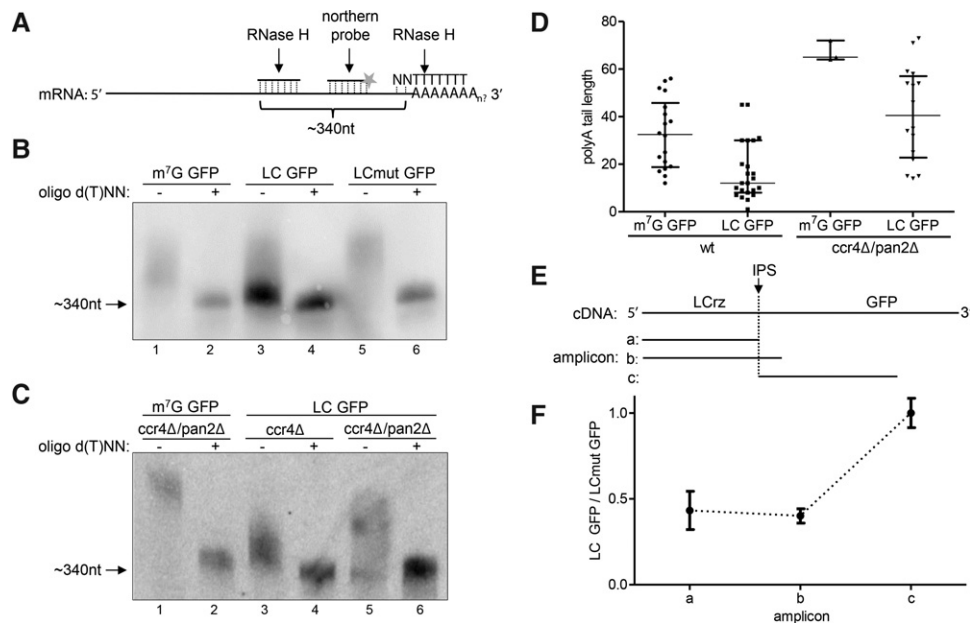
FIGURE 2. Transcripts are lariat-capped cotranscriptionally and processed to have oligo(A) tails. (*A*) Outline of the RNase H assay applied to measure poly(A) tail lengths of GFP mRNAs. Relative positions of the oligo used to cleave the GFP mRNA, the d(T)NN oligo used to trim the poly(A) tail, and the Northern hybridization probe oligo are indicated. (*B*) RNase H/Northern assay of whole cell RNA extracted from wt cells expressing m^{7}G GFP-, LC GFP-, and LCmutGFP-mRNA as indicated. The mobility shift between samples treated without (−) and with (+) oligo d(T)NN indicates the length of the poly(A) tail. (*C*) RNase H/Northern assay of whole cell RNA from cells expressing m^{7}G GFP- or LC GFP-mRNA in the *ccr4Δ* and *ccr4Δpan2Δ* mutant cell backgrounds as indicated. The gel was run at identical conditions and to the same length as in *B* as judged by the xylene cyanol and bromophenol blue dye markers. (*D*) Box-plot showing lengths of poly(A) tails from individual clones of PCR products derived from 3′ RACE experiments of RNA from *B* and *C*. (*E*) Map of amplicons used for nascent RNA analysis by qRT-PCR. Three primer sets were used to generate *amplicon a* located upstream of the IPS (the LCrz processing site), *amplicon b* spanning the IPS, and *amplicon c* targeting the GFP part of the transcript downstream from the IPS. (*F*) qRT-PCR of nascent RNA. All amplicon signals were normalized to that of amplicon c and plotted as the ratio between LC- and LCmut-RNA (uncleaved). The error bars indicate the standard error of the mean (SEM), *n* = 3.

LC-GFP mRNAs, on the other hand, remained oligoadenylated but with slightly longer tails in *ccr4Δ* compared to wt cells (Fig. 2C, lanes 3,4). Moreover, they exhibited a wide distribution of A-tail lengths, ranging from unadenylated or containing few A-residues to tails of intermediate length in the *ccr4Δpan2Δ* double mutant (Fig. 2C, lanes 5,6). This is consistent with redundant deadenylation functions of Pan2p and Ccr4p and suggests that short oligo(A) tails of LC-GFP mRNAs in wt cells derive from deadenylation. Notably, the tail-lengths observed with the LC-GFP mRNA did not reach the same lengths as with m^{7}G-GFP mRNAs in the *ccr4Δpan2Δ* double mutant (Fig. 2C; compare lanes 1 and 5).

To obtain a more precise estimate of poly(A) tail lengths in wt and *ccr4Δpan2Δ* backgrounds, we carried out a modified 3′ RACE experiment based on ligation of adapters to 3′ ends. The poly(A) tail lengths obtained from sequencing of individual 3′ RACE clones are depicted in Figure 2D and agree well with the results in Figure 2B,C. m^{7}G-GFP mRNAs expressed in wt cells harbored a poly(A) tail distribution of 20–60 residues with a median length of 33 compared to a median length of 27 for all mRNAs obtained from a transcriptome-wide sequencing-based characterization (Subtelny et al. 2014). Tails of the few clones obtained from the double mutant background had a median length of 65. As expected,

LC-GFP mRNA poly(A) tail lengths in wt cells fell in two statistically separable groups: one with a median length of 31, probably representing the precursor transcripts, and another with a median length of 10 (range 5–20), representing the processed mRNA equipped with a lariat cap (Fig. 2D). Finally, the LC-GFP mRNA expressed in *ccr4Δpan2Δ* cells exhibited a wide distribution (range 15–71) with a median length of 41. This is consistent with the result from the Northern blot (Fig. 2C, lane 5) and suggests that lariat capping affects the formation of the poly(A) tail in complex ways. Although the oligoadenylated status of the LC-GFP mRNA is eventually the result of redundant deadenylation by Ccr4p and Pan2p, an effect on the initial polyadenylation cannot be ruled out.

LCrz cleaves nascent RNA

To get an idea of the cap status of LC-GFP mRNAs at the time of their 3′ end processing, we analyzed whether cleavage by LCrz might occur cotranscriptionally. To this end, we made chromatin preparations of strains expressing LC-GFP- and LCmut GFP mRNA, respectively, and isolated RNA according to a protocol previously used to characterize nascent RNA (Carrillo Oesterreich et al. 2010). These RNA

preparations contained <4% mature ribosomal RNA and were highly enriched in rRNA precursor and processing intermediate transcripts (Supplemental Fig. S2A,B). Moreover, qRT-PCR analysis showed that unadenylated actin mRNA was enriched more than fivefold in this fraction (Supplemental Fig. S2C). For analysis of GFP reporter constructs we used three different primer sets: (i) one directed toward the LCrz part, (ii) one spanning its cleavage site, and (iii) one directed toward the GFP RNA part (Fig. 2E, amplicons a, b, and c, respectively), and calculated qRT-PCR ratios between experiments with active and inactive LCrz constructs. If LCrz cleaves exclusively after completion of transcription, the ratio of LC-GFP- to LCmut-GFP RNA in the chromatin fraction would expectedly be the same when using all three primer sets. On the other hand, if cleavage occurs cotranscriptionally, qRT-PCR ratios should be lower using the two first primer sets due to uncoupling of 5′- and 3′-end fragments upon cleavage. Indeed, a twofold lower ratio was observed for amplicons a and b compared to c (Fig. 2F), indicating that LCrz cleaves a substantial fraction of transcripts cotranscriptionally. A similar observation was made with a di-cistronic construct with two open reading frames separated by the same LCrz version (data not shown). We favor the notion that LCrz cleavage occurs prior to RNA 3′end cleavage at the poly(A) site. First, the enrichment of unadenylated actin transcripts in the same RNA preparations (Supplemental Fig. S2C) suggests that nascent rather than 3′ processed transcripts are assayed. Second, an RNAPII transcription rate of 30 nt/sec (Mason and Struhl 2005) would allow more than half a minute for the fully transcribed LCrz-containing RNA to fold and cleave. Theoretically, this is ample time considering the fast cotranscriptional folding and cleavage rates observed with ribozymes in vivo (Lai et al. 2013). Thus, we propose that LCrz cleaves nascent transcripts and thus effectively removes the m⁷G cap and the cap-binding complex from the transcribing polymerase.

LC-GFP mRNAs undergo nuclear export

In lariat capping, the transcript diverges from the usual coordinated and cotranscriptional series of processing events that lead to the formation of the mature mRNP and its export. Thus, it could be envisaged that the loss of cap/CBC connectivity would interfere with the export of the LC-GFP mRNA. On the other hand, several reports in budding yeast have shown that cap-less 3′ fragments of transcripts that are produced by bacteriophage polymerases, cleaved by ribozymes or RNaseIII in the nucleus are subsequently found in the cytoplasm (Dower and Rosbash 2002; Meaux and Van Hoof 2006; Meaux et al. 2011). We therefore next determined the cellular localization of the LC-GFP mRNA by a fluorescent in situ hybridization (FISH) experiment with probes targeting the LCrz upstream of the cleavage site and the downstream GFP parts of the mRNA, respectively. Note, that the experiment is complicated by the presence of
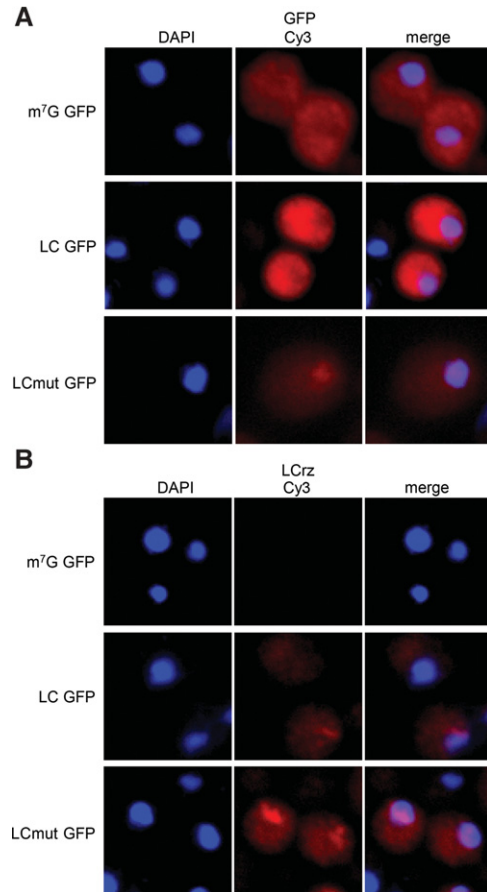

FIGURE 3. The lariat-capped mRNA is exported to the cytoplasm and evenly distributed. (*A*) Fluorescent in situ hybridization (FISH) analysis of cells expressing m⁷G-GFP-, LC-GFP, and LCmut-GFP mRNA, respectively. Representative cells with signals from a Cy3-labeled oligo probe targeting the GFP part of the indicated mRNAs, nuclear staining of cells using DAPI, and a merge of these images are displayed. (*B*) Same as in *A* but using a Cy3-labeled probe targeting the core part of the LCrz.

∼20% of uncleaved precursor LC-GFP mRNA (Fig. 1B). Therefore, we analyzed in parallel the cellular localization of the LCmut-GFP control transcript that differs from the LC-GFP precursor by only a single internal nucleotide in the ribozyme part and thus is expected to behave similarly to the precursor in the FISH experiment. The m⁷G-GFP mRNA showed the expected predominant cytoplasmic signal when using the GFP probe (Fig. 3A, top row) and no staining with the LCrz probe (Fig. 3B, top row). When expressing the LCmut-GFP transcript, the two probes both yielded staining patterns with most cells showing several highly localized and intense signals in the nucleus and a very faint and diffuse signal in the cytoplasm (Fig. 3A,B, bottom rows). The nuclear signals may represent retention of transcripts at chromatin, perhaps at the sites of transcription from the high-copy-number plasmids. The faintness of the cytoplasmic signal is consistent with the expectation that these transcripts are NMD-substrates based on the multiple start and stop signals in the LCrz part of their 5′ UTRs (Supplemental Fig. S1).

Finally, cells expressing the LC-GFP mRNA and hybridized with the GFP probe displayed a faint nuclear signal and a strong, diffuse cytoplasmic signal (Fig. 3A, middle row). Hybridization with the LCrz probe (Fig. 3B, middle row), on the other hand, yielded a staining pattern similar to that of the LCmut-GFP construct, suggesting a large contribution to the signal from the 20% uncleaved precursor. Together, these experiments suggest that the LC-GFP transcript is cleaved in the nucleus and that the 3′ GFP mRNA is exported in its lariat-capped form. We therefore conclude that the lariat-capped mRNAs are exported efficiently to the cytoplasm.

LC-GFP mRNAs are inefficiently translated

Translation of yeast mRNA depends on both its cap and poly(A) tail. Thus, lariat-capped mRNAs with no conventional cap and with only oligoadenylated tails might be compromised in translation. To address this, we performed GFP fluorescence microscopy (Supplemental Fig. S3A) and flow cytometry (Supplemental Fig. S3B) of cells expressing LC-GFP mRNA and compared them to the m^{7}G-GFP and LCmut-GFP controls. Cells harboring the m^{7}G-GFP mRNA were brightly fluorescent in contrast to cells harboring the LCmut-GFP mRNA, which yielded only background autofluorescence. This was also the case for cells harboring a construct having a different ribozyme inactivating mutation (A153G; not shown). Cells expressing LC-GFP mRNA were clearly more fluorescent than the LCmut-GFP control but at levels that were much below that of the m^{7}G-GFP control. Given the high cellular levels of LC-GFP mRNA (Figs. 1B, 3B), this implies that the lariat-capped and oligoadenylated mRNA is inefficiently translated. This conclusion was supported by flow cytometry analysis, which showed that cells expressing LC-GFP mRNA exhibit GFP fluorescence at ~1% of cells expressing m^{7}G-GFP mRNA yet are separable from the background fluorescence of cells expressing LCmut-GFP mRNA (Supplemental Fig. S2B).

In order to isolate the effect of the lariat cap substitution from that of the short oligo(A) tail, we introduced a templated poly(A) tail of 50 nt into the construct. The encoded poly(A) tail was released as part of the mRNA by cleavage using a cotranscribed HDV ribozyme designed to cleave after the last A in the template poly(A) tail and leave a cyclic phosphate end upon cleavage. Because the basic construct relied on polyadenylation within the PGK terminator that is known to harbor several alternative poly(A) sites, we initially made the construct with deletions from the major poly(A) site and upstream into the 3′ UTR. Thus, we tested constructs with full, short, middle length, and long 3′ UTRs, respectively, all with an abrogated major poly(A) site (Fig. 4A). All constructs produced mRNAs of the expected length with approximately the same levels of precursor and lariat-capped products as the construct with the original 3′ UTR (Fig. 4B, top panel). The functionality of the LC and HDV ribozymes was evidenced by detection of the released ribozymes by

Northern blotting analysis (Fig. 4B, middle panels) and the complete absence of HDV extended precursors (data not shown). The absence of a hybridization signal with the HDV probe on the RNA from the construct with a full-length 3′ UTR (Fig. 4B, second panel, lane 3) suggests that a minor poly(A) site upstream HDV was used in this case. Next, we validated the presence of the poly(A) tail on the lariat-capped mRNA with the longest 3′ UTR using the RNase H assay outlined in Figure 2 (Fig. 4C, lanes 1 and 2). This analysis revealed two populations of tails in roughly equal proportions; short tails of variable length as observed with normal polyadenylation, and tails with a defined length consistent with the templated poly(A) tail. A control experiment that removed the precursor transcripts by decapping and 5′ exonuclease treatment prior to the RNase H assay ruled out that the long tails derived from conventionally capped transcripts (Fig. 4C, lanes 3 and 4). The construct was further analyzed by the RNase H assay in a *ccr4Δpan2Δ* background in which the signal representing short tails was absent (Fig. 4D). Thus, we conclude that Pan2p and Ccr4p contribute to the deadenylation of the templated poly(A) tail.

Translation of GFP was monitored by flow cytometry (Fig. 4E, upper part) and the expression of the GFP protein validated by Western blotting analysis (Fig. 4E, lower part). For unknown reasons, the construct with the shortest 3′ UTR did not express GFP. All other constructs with templated poly(A) tails showed fluorescence and GFP protein levels only slightly above that of the LC-GFP construct that produced mRNA with oligoadenylated tails. However, the fluorescence was two orders of magnitude less than with the construct producing conventionally capped and polyadenylated mRNA, and we therefore conclude that lariat-capped mRNAs are translated, albeit at low levels, and that the presence of a templated poly(A) tail has little impact on translation in the absence of a conventional cap.

LC-GFP mRNAs exhibit long half-lives

Cap substitution by lariat capping is presumably a stabilizing modification of mRNA because decapping followed by 5′–3′ decay is the predominant cytoplasmic degradation pathway and because much of the 3′–5′ degradation is dependent on translation competence and thus also indirectly involves the m^{7}G cap (Harigaya and Parker 2012). In addition, the lariat cap is resistant in vitro to yeast debranching enzyme (Nielsen et al. 2005) and the Xrn1p 5′–3′ exonuclease (Fig. 1B; the Ter exonuclease is based on Xrn1p). Conversely, we also considered that the poor translation could stimulate degradation of LC-GFP mRNA. We addressed these questions by estimating the half-life of lariat-capped mRNA. To do this, GFP encoding reporters were placed in a vector where the *GAL1* promoter drives transcription initiation. mRNA half-lives can then be estimated via Northern blotting analysis of the relevant GFP mRNA at different time points
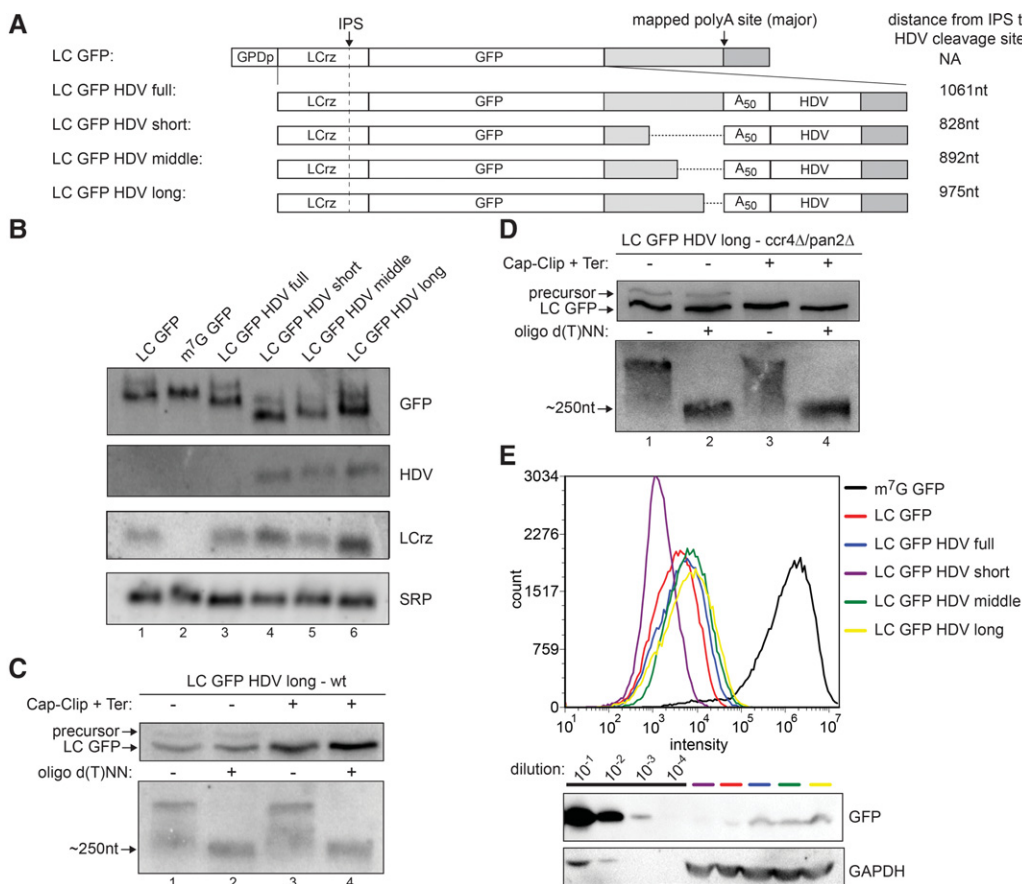
FIGURE 4. The lariat-capped mRNA is inefficiently translated. (*A*) Schematic of constructs with templated poly(A) tails. (*B*) Northern blot analysis using probes against the GFP, HDV, and LCrz parts of the transcript, respectively, as well as SRP RNA (yeast *SCR1*) as a loading control. Only relevant parts of the membrane are shown. (*C*) RNase H/Northern assay of a selected construct expressing a templated poly(A) tail and conducted as described in Figure 2. (*D*) Similar assay conducted with RNA from ccr4Δ/pan2Δ cells. (*E*) Measurements of GFP expression by flow cytometry (*top*) and Western blotting (*bottom*). GAPDH (yeast Tdh3) was used as a loading control.

after suppression of transcription by addition of glucose to the medium. In these experiments, we did not observe precursor transcripts, suggesting that full cleavage by LCrz is obtainable from this construct. The experiments revealed an approximately threefold increase in half-life of the LC-GFP mRNA as compared to the m7G-GFP mRNA (Fig. 5A, upper and middle panels; quantified in Fig. 5B). Importantly, the comparison concerns mRNAs that are predominantly found in the cytoplasm with similarly even distributions (Fig. 3). The addition of a templated poly(A) tail presumably terminating with a 2′, 3′ cyclic phosphate resulting from HDV ribozyme cleavage, did not affect the half-life of the LC-GFP mRNA (Fig. 5A, bottom panel and Fig. 5B). The m7G-capped LCmut-GFP mRNA was almost twofold less stable than the m7G-GFP mRNA and fivefold less stable than the LC-GFP mRNA (Fig. 5A, third panel and Fig. 5B), possibly explaining the steady-state expression levels of the different constructs (Fig. 1B). We conclude that lariat capping of mRNA in yeast results in a significantly increased cytoplasmic stability.

DISCUSSION

Lariat capping in yeast cells

We have expressed a GFP reporter mRNA fused to a lariat capping ribozyme and find that lariat-capped and oligoadenylated GFP mRNA is expressed abundantly in the cytoplasm where it is translated at very low levels. Thus, we have demonstrated successful transfer of LCrz from the myxomycete *Didymium* to yeast. This furthermore rules out an absolute requirement for native cofactors for LCrz function in a cellular environment. It is generally observed that both small cleavage ribozymes, such as the hammerhead (Meaux and Van Hoof 2006; Fong et al. 2009), and HDV ribozymes (Fong et al. 2009), group I (Shin et al. 2004), and group II (Jones et al. 2005) splicing ribozymes retain activity when transferred to other cells and organisms.

Cleavage of the precursor transcript may occur during transcription or after completion of transcription. In its natural setting, the LCrz folds in an inactive conformation
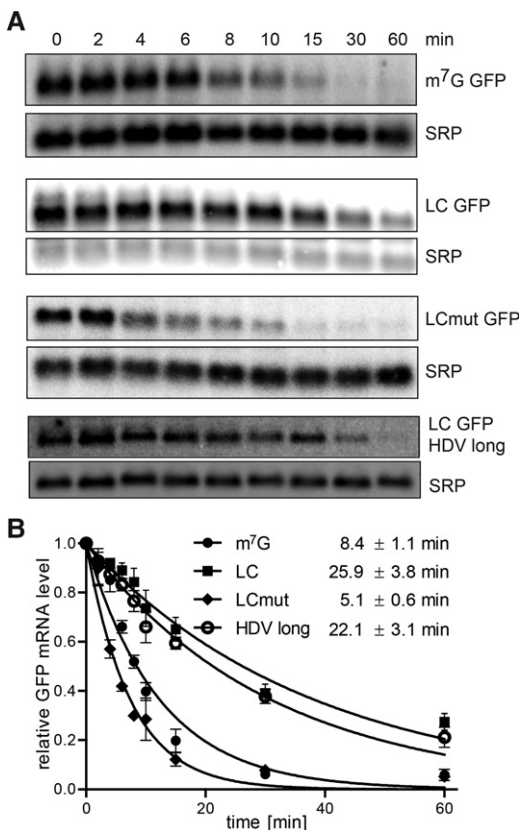
FIGURE 5. Lariat-capped mRNAs show extended half-lives. (*A*) Northern blot analysis of RNA extracted at the indicated time points after glucose suppression of *GAL1* promoter-driven expression. The GFP probe was similar to Figure 1 and an SRP RNA probe (yeast *SCR1*) was used for loading control. (*B*) Quantitation of Northern membranes from *A* and calculation of half-lives based on biological triplicates.

during transcription and is activated at a later stage by a conformational switching mechanism (Nielsen et al. 2008, 2009). In the present construct, essential parts of the inactive conformation have been deleted to promote direct folding into the active conformation. Consistent with this, we observe by analysis of chromatin-associated transcripts that a significant fraction is cleaved during transcription. Even so, the presence of the full-length precursor transcript in the Northern blotting analysis shows that at least a fraction of transcription results in uncleaved transcripts. Based on our experience with LCrz in vitro, we speculate that these are misfolded transcripts that remain uncleaved due to a large energy barrier for refolding into the active conformation. The absence of uncleaved precursors in the half-life experiments, in which a different promoter was used, suggests that full lariat capping is readily attainable. Cotranscriptional cleavage has also been observed with the hammerhead (Meaux and Van Hoof 2006; Fong et al. 2009) and HDV ribozymes (Fong et al. 2009). We conclude that the LCrz in the format used in the present constructs is well accommodated to the gene expression environment in yeast. A previous paper used several variants of LCrz for expression of a homing

endonuclease in yeast. However, this report pre-dated the discovery of the lariat capping activity and has no documentation of the performance of the ribozyme (Decatur et al. 2000).

Lariat capping and pre-mRNA 3′ processing and polyadenylation

The cap structure binds the cap-binding complex (CBC), which recruits factors involved in processing of the nascent transcript (for review, see Gonatopoulos-Pournatzis and Cowling 2014). The cotranscriptional cleavage by the LCrz implies that the connection between the cap and the transcribing polymerase through the nascent RNA strand is lost and this potentially could influence downstream processing events. One of the key processing events is 3′ end cleavage and subsequent polyadenylation of the mRNA. Although it is clear that a substantial fraction of the transcripts are cleaved cotranscriptionally, the timing of the branching reaction is not known. We observe that 3′ processing and polyadenylation in the LC-GFP mRNA occurs at the same site as with m⁷G-GFP mRNA and conclude that the loss of the cap and its associated factors does not interfere with 3′ end processing in the present context. In contrast, it is less clear if lariat capping interferes with polyadenylation. In the double *ccr4Δpan2Δ* mutant, a small fraction of the LC-GFP transcripts appear to have no A-residues added, and the bulk has shorter tails than with the m⁷G-GFP mRNA. This could reflect a defect in polyadenylation or the action of an additional 3′–5′ deadenylase that engages the lariat-capped transcript more efficiently than the conventionally capped transcript. Although there is no evidence for such an exonuclease, candidates exist (e.g., Ngl3p) (Feddersen et al. 2012). Evidence for cap-dependent defects in polyadenylation are scarce (Gonatopoulos-Pournatzis and Cowling 2014 and references herein). An example is that depletion of CBC proteins in HeLa cell nuclear extracts resulted in shorter poly(A) tails upon addition of untailed mRNA substrates (Flaherty et al. 1997). Overall, lariat capping does not seriously interfere with the functional aspects of polyadenylation in the nucleus as evidenced by nuclear stability and efficient export of the LC-GFP mRNA.

Export and localization

Fully matured and packaged mRNPs in yeast are released from the site of transcription and exported upon association with the heterodimeric Mex67-Mtr2 export receptor (for review, see Nino et al. 2013). The export receptor does not bind directly to the mRNA but via export adaptors. The mRNA cap and poly(A) tail does not play a critical role in export although the poly(A) binding proteins Pab1 and Nab2 have both been attributed mRNA export adaptor functions (Hector et al. 2002; Dunn et al. 2005; Iglesias et al. 2010). More specifically, analyses of conditional mutations in the cap guanylation enzyme (*ceg1-ts*) (Fresco and Buratowski

1996) and the cap methyltransferase (*abd1-ts*) (Schwer et al. 2000), demonstrate that there is no accumulation of poly(A) RNA in the nucleus in cap-deficient cells arguing that the m^7G cap is not required for mRNA export in yeast.

Uncleaved LC-GFP pre-mRNA and the LCmut-GFP mRNA both carry an m^7G cap and appear to be retained in the nucleus for unknown reasons. In contrast, the main fraction of LC-GFP mRNA is cleaved and exported with a lariat cap. Thus, the initially added poly(A) tail may help facilitate the export of LC-GFP mRNA. However, it cannot be ruled out that an alternative export pathway is being used or that the export system is leaky. There are several reports demonstrating efficient translocation of the cap-less 3′ cleavage fragment resulting from ribozyme (5′OH) or Rnt1p (5′ P) cleavage (Dower et al. 2004; Meaux and Van Hoof 2006; Meaux et al. 2011), and T7 polymerase transcribed GFP mRNA in yeast carrying a triphosphate 5′ end is cleaved, polyadenylated, and exported to the cytoplasm (Dower and Rosbash 2002). Of particular interest, an m^7G capped and hammerhead ribozyme terminated transcript was rescued for Pab1p association and nuclear export by addition of a transcribed poly(A) tail (Dower et al. 2004) demonstrating the relative importance of the poly(A) tail compared to the m^7G cap for export. Thus, we conclude that the lariat cap is compatible with efficient nuclear export. Once translocated, the LC-GFP mRNA appears to be distributed similarly in the cytoplasm to the m^7G-GFP mRNA, that is, relatively evenly and far from the punctuate distribution seen for, e.g., P-bodies.

Translation and mRNA turnover

The LC-GFP mRNA is expressed at a level comparable to endogenous actin mRNA (data not shown). This is roughly threefold higher than that of the m^7G-GFP mRNA, yet the GFP protein level as evidenced by GFP fluorescence is <1% of GFP protein in the control strain. In yeast, the cap and the poly(A) tail both stimulate translation, and optimal translation requires the presence of both (Meaux and Van Hoof 2006). The inefficient translation of LC-GFP mRNA could be due to the absence of an m^7G cap or to the short oligo (A) tail, or a combination of both. However, introduction of a templated poly(A) tail that could be detected on roughly half of the transcripts had only very minor effects on translation of the LC-GFP mRNA. It has previously been shown that templated poly(A) tails restore Pab1p association to normal levels (Dower et al. 2004), and we therefore conclude that the poly(A) tail by itself contributes marginally to translation. It has previously been shown that the poly(A) tail contributes to 40S recruitment and that capless and polyadenylated mRNAs are translated in yeast extracts (Tarun and Sachs 1995; Preiss and Hentze 1998) and to a lesser degree in spheroblasts (Gallie 1991; Preiss and Hentze 1998). The differences to the situation with LC-GFP mRNA having a templated poly(A) tail could be due to experimental design, in particular the structure of the mRNA, or that our experiments better

reflect the in vivo situation due to the minimal perturbation of the cells. The critical dependence of translation on the presence of the m^7G was expected because failure to methylate the 5′ end guanylate of mRNA at the restrictive temperature in a temperature-sensitive mutant of the cap methyltransferase (*abd1-ts*) resulted in complete shutdown of protein synthesis without massive reduction in steady-state mRNA levels (Schwer et al. 2000).

In yeast, the major mRNA decay pathway consists of deadenylation followed by decapping and 5′–3′ degradation, whereas 3′–5′ degradation by the cytoplasmic exosome appears to be a minor pathway. As outlined above, the poly(A) tails of the lariat-capped mRNAs are eventually shortened into oligo(A) tails by the redundant action of Ccr4p and Pan2p. Once the transcript contains around 10 A residues, the lariat cap appears to provide an efficient block to the decapping step of the major decay pathway. Hence, further decay of the LC-GFP mRNA is most likely due to 3′–5′ degradation by the RNA exosome. Importantly, turnover of lariat-capped mRNA initiates at the normal deadenylation pathway followed by a block resulting in relative stabilization of the transcript. In contrast, failure to guanylate the mRNA 5′ end by interference with the cap guanylation enzyme results in accelerated decay by the 5′ exonuclease Xrn1 as evidenced by analysis of *ceg1-ts* mutants (Schwer et al. 1998). Usage of LCrz constructs may therefore provide a new tool to study decay by the cytoplasmic exosome. For example, it will be of interest to dissect if the cap is directly involved in recruitment of the exosome as has been shown for the nuclear mammalian exosome (Andersen et al. 2013). The switch in degradation pathway from the major pathway to exosomal degradation may be the cause of the observed approximately threefold increase in mRNA half-life. Based on the higher steady-state levels of templated compared to untemplated tails, the removal of the 2′, 3′ cyclic phosphate appeared to constitute an additional rate-limiting step in deadenylation. However, this did not result in a detectably increased half-life of the mRNA. The fate of the trinucleotide lariat cap structure upon degradation of the LC-GFP mRNA is unknown.

Applications of lariat capping

Lariat capping effectively uncouples the normal m^7G cap and associated proteins from the remainder of the mRNP in individual transcript species at conditions where cell growth and morphology appear unaffected. We propose that this provides an experimental tool relevant for different types of studies. First, lariat capping can be used in combination with genetic analysis to dissect the function of the m^7G cap in key cellular processes, examples of which have been demonstrated here. Second, the expression of stable, lariat-capped mRNA with very low translation competence offers at least two applications. These mRNAs could be used to screen for sequence elements that stimulate translation in a cap-independent fashion (Gilbert et al. 2007; Reineke and

Merrick 2009) upon insertion into the 5′ UTR of the mRNA. With the recent discovery of an abundance of di-cistronic transcripts in yeast (Pelechano et al. 2013), many new candidates for such elements might appear. As a screening system for IRES functions, the lariat cap has the advantage compared to conventional di-cistronic reporter systems of excluding the possibility of translational read-through. A second application would be to use the lariat-capped mRNAs as competitors for binding of factors to endogenous mRNAs. Here, it is an advantage, that sequence-identical and lariat-capped versions of any mRNA can readily be designed and expressed. We envisage that such LC-mRNAs could act as decoy targets with minimal effects on other mRNAs and thereby provide important information about the effects of interference with individual mRNA species.

MATERIALS AND METHODS

Plasmids, oligos, and yeast strains

Plasmids, oligos, and *Saccharomyces cerevisiae* strains used in the present study are listed in Supplemental Tables S1, S2, and S3, respectively. The constructs shown in Figure 1A were generated by inserting a fusion of the lariat capping ribozyme Di-166.22 (LCrz) with a GFP reporter gene in the yeast expression vector pG-1 (Guthrie and Fink 2004) using BamHI and SalI/XhoI restriction sites. The insert of the LC GFP HDV full construct shown in Figure 4A was synthesized by GenScript and inserted in the pG-1 vector using same restriction sites as above. The three constructs harboring different lengths of the 3′ UTR were derived from the synthesized insert by PCR amplification using forward primer C1299 and reverse primers C1337, C1338, C1339 for LC GFP HDV-short, -middle, and -long, respectively. The sequences of all the inserts are listed in Supplemental Table S4. The constructs for the half-life experiments were generated by amplifying the relevant inserts from pG-1 constructs using primers C868 and C869 and inserting the amplified PCR products in a pESC-TRP expression vector (Agilent Technologies part number 217453-51) with a *GAL1* promoter using BamHI and XhoI restriction sites.

Growth and transfection

Transformation of yeast strains was performed using LiAc competent cells and salmon sperm DNA as carriers. In brief, 5 mL of cells (OD$_{600}$ below 0.6) grown in YPD medium at 30°C with shaking at 180 rpm were collected, washed in 1× LTE (0.1 M LiAc, 1 mM EDTA, 10 mM Tris–HCl, pH 7.5), resuspended in 60 µL 1× LTE and added to a mixture containing 10 µL of denatured salmon sperm DNA (10 µg/µL), 2 µL of plasmid DNA (250 ng/µL), 60 µL 5× LTE and 240 µL 50% PEG3340. The cells were incubated at 30°C for 30 min followed by a 13 min heat shock at 42°C. Then, the cells were collected by centrifugation, resuspended in 200 µL sterile H$_2$O and plated on selection plates. Transformed yeast cells were grown overnight in synthetic dropout medium depleted for tryptophan (SC-Trp medium, Sigma-Aldrich Y1876), diluted the following day and harvested at OD$_{600}$ = 0.7–1.0 depending on the downstream analysis.

RNA extraction and nascent RNA preparation

Whole cell RNA was extracted using hot phenol. In brief, fresh cell pellets were incubated in 1 volume of TES buffer (10 mM EDTA, 0.5% SDS, 10 mM Tris–HCl, pH 7.5) and 1 volume acidic phenol (pH 4.5) at 65°C with shaking for 1 h. The RNA was extracted twice in phenol and twice in chloroform followed by ethanol precipitation. Chromatin for nascent RNA preparation was extracted according to Carrillo Oesterreich et al. (2010). The chromatin pellet was resuspended in 1× DNase I buffer, incubated with 5 U of DNase I (Fermentas) for 30 min at 37°C and subsequently for 1 h at 37°C after addition of 2 µL of Proteinase K (20 mg/mL) (Fermentas). The nascent RNA preparation was extracted twice in acid phenol and twice in chloroform, followed by incubation with 2 U of DNase I for 20 min at 37°C to remove any trace of DNA. The quality of the nascent RNA was assessed on an Agilent Bioanalyzer, and the RNA was subsequently validated for the content of nascent RNA by comparing the ratios between precursor-specific amplicons and 18S rRNA amplicons in chromatin-associated and whole cell RNA, as well as comparing the ratio of actin mRNA made from cDNA synthesized with either d(T)or oligo dN6 primers between chromatin-associated RNA and whole cell RNA. First-strand cDNA was synthesized with either dN6 or oligo d(T) primers using Superscript III (Life Technologies) according to the manufacturer. The cDNA was diluted 50× and used for qPCR analysis on a LightCycler Nano System (Roche) using FastStart Essential DNA Green Master reaction mixture according to the manufacturer.

5′ end probing by TAP (Cap-Clip)/Terminator treatment and Northern blotting analysis

Aliquots of whole cell RNA (10 µg) were treated in parallel with or without enzyme. For TAP treatment the RNA was incubated with 5 U of Tobacco Acid Pyrophosphatase (Epicentre) according to the manufacturer. Subsequently, the RNA was extracted using phenol–chloroform–isoamyl alcohol (PCI) and ethanol precipitated, resuspended in DEPC H$_2$O, and then incubated with 1 U of Terminator 5′-phosphate-dependent exonuclease (Epicentre) at 30°C for 60 min. The RNA was then separated by gel electrophoresis on a 1% denaturing agarose gel. The integrity of the RNA was assessed by ethidium bromide staining and the RNA subsequently transferred to a positive charged nylon membrane (BrightStar-Plus, Ambion), using the capillary blotting method, followed by UV cross-linking. The probes (10 pmol each) were labeled with [γ-^{32}P]ATP using T4 polynucleotide kinase (Fermentas) and hybridized to the membrane in hybridization buffer (4× Denhardts solution, 6× SSC, 0.1% SDS). The membrane was then washed four times in washing buffer (3× SSC, 0.1% SDS) and exposed to a Phosphor Imager Screen and analyzed by ImageQuant software. During the project TAP was discontinued by Epicentre and the TAP enzyme was replaced with Cap-Clip Acid Pyrophosphatase (CellScript) and used according to the manufacturer.

Primer extension analysis

Whole cell RNA (1 µg) was incubated in 6 µL 1× RevertAid reverse transcriptase buffer (Thermo Scientific) containing 1 pmol of oligo C723 (labeled with [γ-^{32}P]ATP) at 90°C for 1 min, followed by incubation at 42°C for 10 min. The mixture was added to a 4 µL

solution consisting of 0.5 mM dNTP, 1× RevertAid RT buffer, and 40 U of RevertAid RT and further incubated at 42°C for 30 min. The sequencing ladder was made by sequencing 400 ng of plasmid DNA (GPDp-LCwt GFP) with 1 pmol of radiolabeled oligo C723 using the Thermo Sequenase Cycle sequencing Kit (USB) according to the manufacturer. The primer extension reaction and the sequencing ladder were run on an 8% polyacrylamide/50% urea gel.

RNase H assay for poly(A) tail analysis

Whole cell RNA (5 μg) was incubated in 1× RNase H buffer with 2.5 U of RNase H (New England Biolabs) for 1 h at 37°C in the presence of 25 pmol oligo C1021 with or without 225 pmol of oligod(T)NN. Subsequently, the RNA was separated on an 8% polyacrylamide/50% urea gel, transferred to a membrane by electroblotting, UV cross-linked, and a radiolabeled oligo probe (C1022) was hybridized to the membrane as described above.

3′ RACE and sequencing for poly(A) tail length analysis

One hundred picomoles of an RNA oligo (CR22b) with 5′ monophosphate and 3′ddC ends was ligated to 2 μg of whole cell RNA in a 10 μL 1× T4 RNA ligase I buffer (NEB) supplemented with 1 mM ATP, 1 mM hexamine cobalt chloride, 20% PEG8000, and 10 U of T4 RNA ligase I (NEB). The mixture was incubated at 16°C overnight followed by the addition of 40 μL 1× TE buffer and 150 μL DEPC H_2O. Then, the RNA was extracted with PCI and ethanol precipitated in the presence of 5 μg glycogen and resuspended in DEPC H_2O followed by first-strand cDNA synthesis with 25 pmol DNA oligo (C959) using Superscript III (Life Technologies). The cDNA synthesis was performed at 50°C for 1 h followed by incubation with 2.5 U of RNase H for 20 min at 37°C. cDNA (1 μL) was amplified by PCR with oligos C1031 and C959 using Taq polymerase (Fermentas) in the presence of 3 mM $MgCl_2$. The 3′RACE products generated by the PCR were cloned into pCR-4 TOPO TA vector using the TOPO TA Cloning Kit (Life Technologies) and transfected into *E. coli* DH5α. Colony PCR using Taq polymerase (Fermentas) with oligos C1031 and C959 was performed on single colonies, and 1 μL of the PCR products were subsequently treated with 5 U of Exonuclease I and 0.25 U of FastAP (Thermo Scientific) prior to sequencing with C1031 using the BigDye Terminator v1.1 Cycle Sequencing Kit according to the manufacturer. The sequencing reactions were analyzed on an ABI 3130XL Genetic Analyzer, and data handling was performed using Sequencing Analysis 5.2 software (Applied Biosystems). The sequences were aligned using the BioEdit Sequence Alignment Editor.

FISH analysis of mRNA localization

The protocol for FISH analysis was according to Schmid et al. (2015). Briefly, cells were fixed in 3.8% paraformaldehyde for 1 h, washed twice, resuspended in 1.2 M sorbitol/0.1 M K_2HPO_4 and adhered to poly-L-lysine treated 14-well slides (Immuno-Cell Int.) using mounting solution containing DAPI (Life Technologies). RNAs were detected using a mixture of Cy3-labeled oligonucleotide probes (T* represents amino-allyl-C6 modified dT): AT*TAAGTG TTCAACCCGAT*TGCATCATGGTGAT*TAGCCATGATACTT*C, GT*TAGGACGGATGTT*ACGGGATCGTCCCCCACCGT*TTT

AACCCAATT*A for LCrz and GT*GCCCATTAACAT*CACCAT CTAATT*CAACAAGAAT*TGGGACAACT*CCAGT, GTACAT*AA CCTTCGGGCAT*GGCACTCTT*GAAAAAGTCAT*GCCGTTTCA T*AT, GATTCCAT*TCTTTTGTT*TGTCTGCCAT*GATGTATAC AT*TGTGTGAGTT*ATA, CCCAGCAGCT*GTTACAAACT*CAAG AAGGACCAT*GTGGTCT*CTCTTTTCGT*T, for GFP, respectively.

Image manipulations were performed using ImageJ software.

Fluorescence microscopy and flow cytometry

Cells were washed twice and resuspended in 1× PBS. For microscopy, cells were mounted on glass slides, and GFP was detected using a Leica DM 4000B microscopy equipped with a Leica DC300FX digital camera. Cells for flow cytometry were diluted in 1× PBS to a concentration of 10^3 cells per μL. 5×10^4 cells were counted in a gating excluding cell debris and dead cells on an Accuri C6 flow cytometer equipped with CFlow sampler analysis software using fast sampling rate mode, with FSC-H threshold of 40,000 and 530/30 nm filter.

Western blotting analysis

Yeast culture (3 mL) ($OD_{600} = 0.7$) was collected by centrifugation at 3000g for 1 min, then washed in 200 μL sterile H_2O followed by incubation in 200 μL of 0.1 M NaOH for 5 min at room temperature. Subsequently, the cells were collected and resuspended in 40 μL of 1× SDS (62.5 mM Tris–HCl, pH 6.8, 2.5% SDS, 0.002% bromophenol blue, 0.7135 M (5%) β-mercaptoethanol, 10% glycerol) and lysed by incubation for 5 min at 95°C. Cell debris was collected by centrifugation at 10,000g for 3 min, and 25 μL of the cell lysate was loaded on a 10% SDS-PAGE and separated for 2 h at 110 V. Proteins were transferred to a nitrocellulose membrane (Amersham Bioscience) in 1× NuPAGE Transfer buffer supplemented with 10% ethanol for 55 min at 50 V (XCell II Blot Module, Life Technologies). Unoccupied membrane binding sites were subsequently blocked for 60 min in Tris-buffered saline supplemented 0.1% Tween 20 (P1379, Sigma-Aldrich) (TBST) and 5% skim milk powder (70166, Sigma-Aldrich). The membrane was subsequently washed three times in TBST and incubated at 4°C for 24 h with primary antibodies diluted in TBST supplemented with 5% bovine serum albumin (A4503, Sigma-Aldrich). For GFP, mouse anti-GFP antibody was used (8371-2, Clontech) in a 1:2000 dilution. For GAPDH, rabbit anti-GAPDH antibody (Ab9485, Abcam) was used in a 1:5000 dilution. The membrane was washed, and proteins visualized following 60 min incubation at room temperature with secondary HRP-rabbit anti-mouse Ig (for GFP) (P0260, Dako) and secondary HRP-swine anti-rabbit Ig (for GAPDH) (P0399, Dako) using ECL technology (RPN2232, Amersham Biosciences).

mRNA half-life measurements

For half-life experiments, the GFP mRNA was expressed from a GAL1 promoter in a pESC-TRP expression vector. Yeast cells grown in SC-Trp medium supplemented with 2% galactose (Sigma-Aldrich G0750) were collected at $OD_{600} = 0.4$, resuspended in 30°C warm SC-Trp medium, and immediately supplemented with glucose to a final concentration of 2% (equal to time point 0 min). Samples taken at each time point were snap cooled to 0°C in liquid nitrogen, collected by centrifugation followed by removal of the medium, and pellets

were frozen in liquid nitrogen and stored at −80°C. RNA extraction and Northern blotting was performed as described above.

SUPPLEMENTAL MATERIAL

Supplemental material is available for this article.

REFERENCES

Andersen PR, Domanski M, Kristiansen MS, Storvall H, Ntini E, Verheggen C, Schein A, Bunkenborg J, Poser I, Hallais M, et al. 2013. The human cap-binding complex is functionally connected to the nuclear RNA exosome. *Nat Struct Mol Biol* **20:** 1367–1376.

Brown CE, Sachs AB. 1998. Poly(A) tail length control in *Saccharomyces cerevisiae* occurs by message-specific deadenylation. *Mol Cell Biol* **18:** 6548–6559.

Carrillo Oesterreich F, Preibisch S, Neugebauer KM. 2010. Global analysis of nascent RNA reveals transcriptional pausing in terminal exons. *Mol Cell* **40:** 571–581.

Decatur WA, Einvik C, Johansen S, Vogt VM. 1995. Two group I ribozymes with different functions in a nuclear rDNA intron. *EMBO J* **14:** 4558–4568.

Decatur WA, Johansen S, Vogt VM. 2000. Expression of the *Naegleria* intron endonuclease is dependent on a functional group I self-cleaving ribozyme. *RNA* **6:** 616–627.

Dower K, Rosbash M. 2002. T7 RNA polymerase-directed transcripts are processed in yeast and link 3′ end formation to mRNA nuclear export. *RNA* **8:** 686–697.

Dower K, Kuperwasser N, Merrikh H, Rosbash M. 2004. A synthetic A tail rescues yeast nuclear accumulation of a ribozyme-terminated transcript. *RNA* **10:** 1888–1899.

Dunn EF, Hammell CM, Hodge CA, Cole CN. 2005. Yeast poly(A)-binding protein, Pab1, and PAN, a poly(A) nuclease complex recruited by Pab1, connect mRNA biogenesis to export. *Genes Dev* **19:** 90–103.

Feddersen A, Dedic E, Poulsen EG, Schmid M, Van LB, Jensen TH, Brodersen DE. 2012. *Saccharomyces cerevisiae* Ngl3p is an active 3′-5′ exonuclease with a specificity towards poly-A RNA reminiscent of cellular deadenylases. *Nucleic Acids Res* **40:** 837–846.

Flaherty SM, Fortes P, Izaurralde E, Mattaj IW, Gilmartin GM. 1997. Participation of the nuclear cap binding complex in pre-mRNA 3′ processing. *Proc Natl Acad Sci* **94:** 11893–11898.

Fong N, Ohman M, Bentley DL. 2009. Fast ribozyme cleavage releases transcripts from RNA polymerase II and aborts co-transcriptional pre-mRNA processing. *Nat Struct Mol Biol* **16:** 916–922.

Fresco LD, Buratowski S. 1996. Conditional mutants of the yeast mRNA capping enzyme show that the cap enhances, but is not required for, mRNA splicing. *RNA* **2:** 584–596.

Gallie DR. 1991. The cap and poly(A) tail function synergistically to regulate mRNA translational efficiency. *Genes Dev* **5:** 2108–2116.

Gilbert WV, Zhou K, Butler TK, Doudna JA. 2007. Cap-independent translation is required for starvation-induced differentiation in yeast. *Science* **317:** 1224–1227.

Gonatopoulos-Pournatzis T, Cowling VH. 2014. Cap-binding complex (CBC). *Biochem J* **457:** 231–242.

Guthrie C, Fink GR, ed. 2004. *Guide to yeast genetics and molecular and cell biology, part A. Meth Enzymol* **194**. Elsevier Academic Press, San Diego, CA.

Harigaya Y, Parker R. 2012. Global analysis of mRNA decay intermediates in *Saccharomyces cerevisiae*. *Proc Natl Acad Sci* **109:** 11764–11769.

Hector RE, Nykamp KR, Dheur S, Anderson JT, Non PJ, Urbinati CR, Wilson SM, Minvielle-Sebastia L, Swanson MS. 2002. Dual requirement for yeast hnRNP Nab2p in mRNA poly(A) tail length control and nuclear export. *EMBO J* **21:** 1800–1810.

Iglesias N, Tutucci E, Gwizdek C, Vinciguerra P, Von Dach E, Corbett AH, Dargemont C, Stutz F. 2010. Ubiquitin-mediated mRNP dynamics and surveillance prior to budding yeast mRNA export. *Genes Dev* **24:** 1927–1938.

Johansen SD, Haugen P, Nielsen H. 2007. Expression of protein-coding genes embedded in ribosomal DNA. *Biol Chem* **388:** 679–686.

Jones JP III, Kierlin MN, Coon RG, Perutka J, Lambowitz AM, Sullenger BA. 2005. Retargeting mobile group II introns to repair mutant genes. *Mol Ther* **11:** 687–694.

Lai D, Proctor JR, Meyer IM. 2013. On the importance of cotranscriptional RNA structure formation. *RNA* **19:** 1461–1473.

Long MB, Jones JP III, Sullenger BA, Byun J. 2003. Ribozyme-mediated revision of RNA and DNA. *J Clin Invest* **112:** 312–318.

Mason PB, Struhl K. 2005. Distinction and relationship between elongation rate and processivity of RNA polymerase II in vivo. *Mol Cell* **17:** 831–840.

Meaux S, Van Hoof A. 2006. Yeast transcripts cleaved by an internal ribozyme provide new insight into the role of the cap and poly(A) tail in translation and mRNA decay. *RNA* **12:** 1323–1337.

Meaux S, Lavoie M, Gagnon J, Abou Elela S, van Hoof A. 2011. Reporter mRNAs cleaved by Rnt1p are exported and degraded in the cytoplasm. *Nucleic Acids Res* **39:** 9357–9367.

Meyer M, Nielsen H, Olieric V, Roblin P, Johansen SD, Westhof E, Masquida B. 2014. Speciation of a group I intron into a lariat capping ribozyme. *Proc Natl Acad Sci* **111:** 7659–7664.

Nielsen H, Westhof E, Johansen S. 2005. An mRNA is capped by a 2′, 5′ lariat catalyzed by a group I-like ribozyme. *Science* **309:** 1584–1587.

Nielsen H, Beckert B, Masquida B, Johansen SD. 2008. The GIR1 branching ribozyme. In *Ribozymes and RNA catalysis* (ed. Lilley DMJ, Eckstein F), pp. 229–252. Royal Society of Chemistry, London, UK.

Nielsen H, Einvik C, Lentz TE, Hedegaard MM, Johansen SD. 2009. A conformational switch in the DiGIR1 ribozyme involved in release and folding of the downstream I-DirI mRNA. *RNA* **15:** 958–967.

Nino CA, Herissant L, Babour A, Dargemont C. 2013. mRNA nuclear export in yeast. *Chem Rev* **113:** 8523–8545.

Pelechano V, Wei W, Steinmetz LM. 2013. Extensive transcriptional heterogeneity revealed by isoform profiling. *Nature* **497:** 127–131.

Preiss T, Hentze MW. 1998. Dual function of the messenger RNA cap structure in poly(A)-tail-promoted translation in yeast. *Nature* **392:** 516–520.

Ramanathan A, Robb GB, Chan SH. 2016. mRNA capping: biological functions and applications. *Nucleic Acids Res* **44:** 7511–7526.

Reineke LC, Merrick WC. 2009. Characterization of the functional role of nucleotides within the URE2 IRES element and the requirements for eIF2A-mediated repression. *RNA* **15:** 2264–2277.

Schmid M, Olszewski P, Pelechano V, Gupta I, Steinmetz LM, Jensen TH. 2015. The nuclear polyA-binding protein Nab2p is essential for mRNA production. *Cell Rep* **12:** 128–139.

Schwer B, Mao X, Shuman S. 1998. Accelerated mRNA decay in conditional mutants of yeast mRNA capping enzyme. *Nucleic Acids Res* **26:** 2050–2057.

Schwer B, Saha N, Mao X, Chen HW, Shuman S. 2000. Structure-function analysis of yeast mRNA cap methyltransferase and high-copy suppression of conditional mutants by AdoMet synthase and the ubiquitin conjugating enzyme Cdc34p. *Genetics* **155:** 1561–1576.

Shin KS, Sullenger BA, Lee SW. 2004. Ribozyme-mediated induction of apoptosis in human cancer cells by targeted repair of mutant p53 RNA. *Mol Ther* **10:** 365–372.

Subtelny AO, Eichhorn SW, Chen GR, Sive H, Bartel DP. 2014. Poly(A)-tail profiling reveals an embryonic switch in translational control. *Nature* **508:** 66–71.

Sullenger BA, Gilboa E. 2002. Emerging clinical applications of RNA. *Nature* **418:** 252–258.

Tang Y, Nielsen H, Birgisdottir AB, Johansen S. 2011. A natural fast-cleaving branching ribozyme from the amoeboflagellate *Naegleria pringsheimi*. *RNA Biol* **8:** 997–1004.

Tang Y, Nielsen H, Masquida B, Gardner PP, Johansen SD. 2014. Molecular characterization of a new member of the lariat capping twin-ribozyme introns. *Mobile DNA* **5:** 25.

Tarun SZ Jr, Sachs AB. 1995. A common function for mRNA 5′ and 3′ ends in translation initiation in yeast. *Genes Dev* **9:** 2997–3007.

Topisirovic I, Svitkin YV, Sonenberg N, Shatkin AJ. 2011. Cap and cap-binding proteins in the control of gene expression. *Wiley Interdiscip Rev RNA* **2:** 277–298.

Tucker M, Valencia-Sanchez MA, Staples RR, Chen J, Denis CL, Parker R. 2001. The transcription factor associated Ccr4 and Caf1 proteins are components of the major cytoplasmic mRNA deadenylase in *Saccharomyces cerevisiae*. *Cell* **104:** 377–386.

Vader A, Nielsen H, Johansen S. 1999. In vivo expression of the nucleolar group I intron-encoded I-DirI homing endonuclease involves the removal of a spliceosomal intron. *EMBO J* **18:** 1003–1013.